# OPTIMIZATION OF SRF LINACS*

Tom Powers, JLAB, Newport News, VA, 23606 USA

*Abstract*

This work describes preliminary results of a new software tool that allows one to vary parameters and understand the effects on the optimized costs of construction plus 10 year operations of an SRF linac, the associated cryogenic facility, and controls, where operations includes the cost of the electrical utilities but not the labor or other costs. It derives from collaborative work done with staff from Accelerator Science and Technology Centre, Daresbury, UK several years ago while they were in the process of developing a conceptual design for the New Light Source project [1]. The initial goal was to convert a spreadsheet format to a graphical interface to allow the ability to sweep different parameter sets. The tools also allow one to compare the cost of the different facets of the machine design and operations so as to better understand the tradeoffs. The work was first published in an ICFA Beam Dynamics Newsletter [2]. More recent additions to the software include the ability to save and restore input parameters as well as to adjust the $Q_0$ versus E parameters in order to explore the potential costs savings associated with doing so. Additionally, program changes now allow one to model the costs associated with a linac that makes use of energy recovery mode of operation.

## INTRODUCTION

Every well-designed machine goes through the process of cost optimization several times during its design, production and operation. The initial optimizations are done during the early proposal stage of the project when none of the systems have been engineered. When a superconducting radio frequency (SRF) linac is implemented as part of the design, it is often a difficult decision as to the frequency and gradient that will be used. Frequently, such choices are made based on existing designs, which invariably necessitate moderate to substantial modifications so that they can be used in the new accelerator. Thus the problem with using existing designs is that they will frequently provide a higher cost machine or a machine with sub-optimal beam physics parameters.

## SOFTWARE DESCRIPTION

The software is written in LabView programming language, which is a graphical user interface language typically used for instrumentation and control. It is structured as state machine which allows one to add and remove functionality as necessary. The language is also suited for developing straightforward user interface.

### *Input – Output Parameters*

A detailed list of the input parameters is given in Table 1. There are two general terms for cryogenic losses. The first is static losses associated with each of the SRF cryomodules, transfer lines, etc. and RF driven, or dynamic, losses which is determined on a cavity by cavity basis. The static heat losses include the losses in the cryomodule, its associated valve box, and per kilometer transfer line losses. These are user inputs to the program. $Q_0$ losses are determined based on the cavity geometry, operating temperature, material type and processing techniques which are all input variables to the program. Figure 1 shows the user interface for the input variables.

Table 1: Input Parameters List

| **SRF Parameters** | *Baseline Costs* |
|---|---|
| Final Linac Energy (GeV) | Cryomodule Cost ($M/unit) |
| Gradient (V/m) | RF Power ($/W) |
| Frequency (Hz) | RF Control, etc. ($k/Cavity) |
| Cavities Per Cryomodule | Inter CM Girder ($k/unit)[3] |
| Active Length Per Cavity (m) | Tunnel Civil ($k/m) |
| Packing Factor Tot L/Active L | AC Power ($/MW-Hour) |
| Normalized Shunt Imp. (Ω/m) | 5kW @ 2K Plant ($M) |
| $B_{PEAK}/E_{ACC}$ (mT/(MV/m)) | 5kW Plant Civil ($M) |
| Geometry Factor (Ω) | Transfer Line ($k/m) |
| Beam Current (A) | 2K Plant Margin |
| Beam Phase (deg) | % Inc. Plant Cost @1.8K |
| Detune Freq. Budget (Hz) | Linac R&D Cost ($M) |
| RF Power Margin | RF Wall Plug Eff. |
| Operating Temperature (K) | Cntrl. AC Pwr/Girder (kW) |
| Maximum Loaded-Q | Operations Week |
| Loaded-Q Uncertainty | Power Overhead[4] |
| Material and Treatment[1] | Static Heat Load/CM (W)[5] |
| Beam Transient Handling[2] | Transfer Line Heat (W/km) |
| $Q_0$ Improvement | |
| $Q_0$ Slope Adjust | |
| ERL Effective Beam Current | |
| ERL Effective Beam Phase | |
| ERL Tune Beam | |

Notes from Table 1:

1. A combination of materials and treatments were modeled in the $Q_0$ calculations. These were permutations of fine grain niobium and large grain niobium and vacuum baked at 120°C or not.

* Authored by Jefferson Science Associates, LLC under U.S. DOE Contract No. DE-AC05-06OR23177. The U.S. Government retains a non-exclusive, paid-up, irrevocable, world-wide license to publish or reproduce this manuscript for U.S. Government purposes.

2. The phase of the beam current can have a substantial impact on optimizing the loaded-Q and RF power requirements in an SRF cavity [3]. Under certain circumstances the RF power requirements are substantially higher for short periods of time. There are techniques which can be used to compensate for said transients, such as slowly ramping up the beam current while the cavity tuners operate.
3. The inner cryomodule girder is the vacuum hardware, beam diagnostics hardware, and magnets that make up the common beam line hardware set between cryomodules. Also included in this item are the controls electronics and magnet power supplies.
4. The power overhead in the baseline costs column includes items such as lighting, HVAC, and cooling tower power. An increase of 25% over the calculated electrical demand was used for this parameter.
5. The static heat load per cryomodule included the losses in the cryomodule as well as the associated valve boxes.

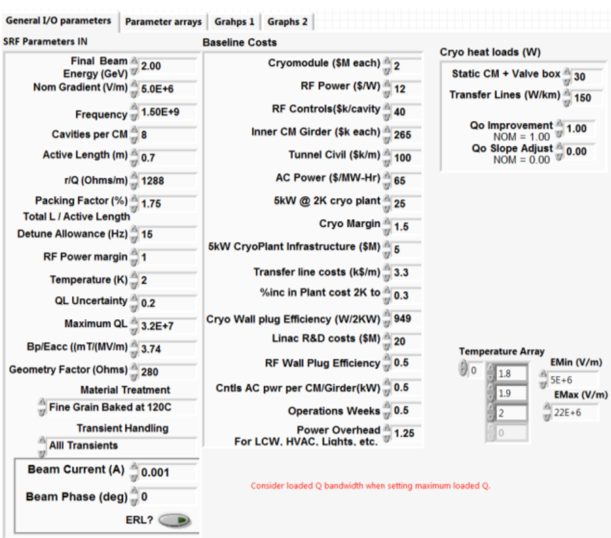


Figure 1: User input screen for the majority of the input variables.

The output parameters include items such as the total construction costs, operating costs, SRF parameters. They are calculated for each value of the swept input variable. They are available in the form of graphs as well as in a text file. Table 2 contains a listing of the output variables that are currently in the program. Figure 2 shows a typical graphical interface with pull down menu shown for one of the graphs.

*Calculating $Q_0$*

$Q_0$ is calculated for each data point, and is based on a compilation of historic data. This historical data is a compilation from measurements taken in the vertical test area at Jefferson Lab, where, over the past 20 years staff have performed more than 4200 tests on superconducting cavities of various configurations and frequencies. A series of curve fits were done on a subset of these data in

Table 2: Output Parameter List

| Outputs |
|---|
| Total Construction Plus Operating Costs ($M) |
| Construction Costs ($M) |
| Cryogenic Plant Costs ($M) |
| Cryomodules Costs ($M) |
| Inner Cryomodule Girder Costs ($M) |
| Accelerator Tunnel, and Service Building Civil Construction Costs ($M) |
| 10 Year Power Costs ($M) |
| Linac Total Length (m) |
| Number of Cryomodules |
| Number of Cavities |
| Number of Inner Cryomodule Girders |
| Individual Cryomodule Dynamic Heat (W) |
| Linac 2K Heat Load (W) |
| 2K Heat Load With Margin |
| $Q_0$ |
| Matched Loaded-Q |
| RF Power Per Cavity (kW) |
| Cryo AC Power (MW) |
| Non-Cryo AC Power (MW) |

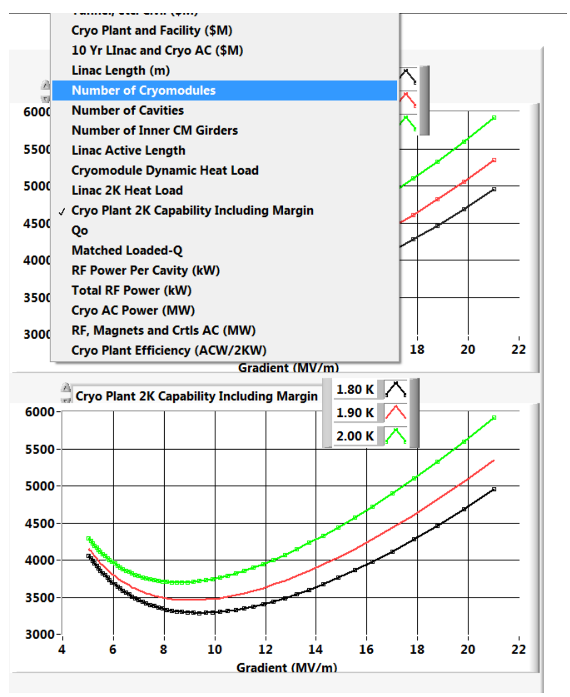


Figure 2: Typical output plots and selector control for plots.

order to determine a $Q_0$ value as a function of gradient, frequency and operating temperature [4]. The analysis was limited in a number of areas due to a lack of completed data sets. The analysis did take into account low to mid-field Q-slope as well as the basic material parameters, cavity shapes, etc. It does not take into account high field slope which is an area that is currently undergoing revision. Another area that is under review is $Q_0$ degradation between vertical test and cryomodule installation in the accelerator, as well as long term degradation of the $Q_0$ in operational conditions. Figure 3, shows the value of $Q_0$ as a function of frequency at 16 MV/m at three different temperatures. For this data the cavity models used had the same geometry factor, and ratio of peak magnetic field to average electric field as the CEBAF low loss cavities used in the 12 GeV upgrade.

Provisions have been added to the program to scale $Q_0$ in two ways. The first is to simply multiply $Q_0$ by the "$Q_0$ improvement factor." The second is to adjust the slope of the $Q_0$ as a function of accelerating gradient. While the former is straightforward the latter is matter of adjustment by trial and error.

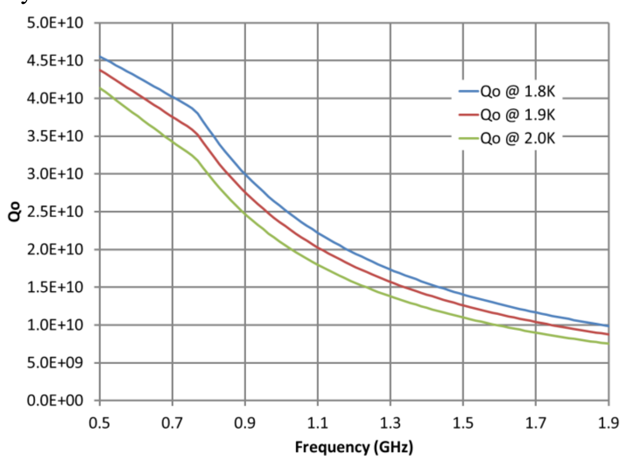


Figure 3: $Q_0$ as a function of frequency and temperature at 16 MV/m. All frequencies scaled from CEBAF C100 upgrade cavity.

## *Calculating Loaded-Q and RF Power*

The matched loaded-Q is the loaded-Q such that the installed RF power is minimized. As discussed in the Input/Output Parameters section, the selected loaded-Q values depend on the whether the RF power can maintain gradient regulation under all transient beam loading conditions or only in a steady-state condition. Equation (1) provides the matched loaded-Q value under all transient conditions, while Equation (2) gives the matched loaded-Q value under steady state conditions.

$$Q_L\big|_{MinPower} = \frac{E}{\sqrt{\left(I_0(r/Q)\cos\psi_B\right)^2 + \left(\pm 2\frac{\delta f}{f_0}E + I_0\,(r/Q)\sin\psi_B\right)^2}} \quad (1)$$

$$Q_L\big|_{MinPower} = \frac{E}{\sqrt{\left(I_0(r/Q)\cos\psi_B\right)^2 + \left(\pm 2\frac{\delta f}{f_0}E\right)^2}} \quad (2)$$

Here, $E$ is the gradient in V/m, $I_0$ is the effective beam current in amperes, *(r/Q)* is the normalized shunt impedance in Ohms/m, $\psi_B$ is the phase of the beam current relative to the cavity gradient, $\delta f$ is the difference between the RF frequency and $f_0$ which is the resonant frequency of the cavity [5].

Once the matched loaded-Q is determined, it is used along with the detune frequency budget, the uncertainly in the loaded-Q and the remainder of the cavity parameters to calculate the permutations on the forward power necessary for operation at each point. The maximum value of this data set is used as the minimum RF power required. This is multiplied by the RF power margin to determine the RF power per cavity. There is no margin in the RF power for cavities operated above the design value, which is an area for future modifications to the program.

## *Cryogenic System Costs*

The baseline plant and infrastructure costs that were used were that of the 5 kW at 2 K plant that was built as part of the CEBAF 12 GeV upgrade [6]. One major assumption is that the ratio of 50 K shield power to 2 K power is similar to that in CEBAF. Another critical aspect of the actual costs is that the plant was designed by, major components procured by, and the system integrated by Jefferson Lab staff. Were the plant to be procured as a turn-key plant the costs would likely be significantly higher. The procurement, installation and commissioning costs scaling is given in Equation (3)

$$Cost_{Power} = Cost_{2.05K}\left(\frac{Power_{2.05K}}{5{,}000}\right)^{0.7} \quad (3)$$

Where $Cost_{Power}$ is the overall cost of a 2.05 K plant at $Power_{2.05K}$, and $cost_{2.05K}$ is sum of the two input cost parameters of 5kW at 2K Plant costs and 5kW Plant Civil costs.

The wall plug efficiency, being the ratio of the total AC power divided by the 2.05 K power, was determined by plotting the efficiency achieved by several existing plants used at accelerators [7] and generating a third order fit between 800 W and 5 kW at 2 K. It includes all AC power including warm compressors. Cooling towers, HVAC, lighting, etc. are included as part of a separate line item based on the overall power budget. The plant cost was increased linearly by 30% between 2.05 K and 1.8 K [5]. It should be noted that these are just estimates and it is critical that any final design of the cryogenic plant be closely coordinated with the design of the cryomodules in order to optimize the overall cost. [8, 9].

There are two factors to consider when adjusting the wall plug efficiency between 2.05 K and 1.8 K. The first is the temperature effect on the Carnot work. This goes as the ratio of the two temperatures and increases the wall plug power by 14% when the temperature is reduced from 2.05 K to 1.8 K. The second is the change in the Carnot efficiency which goes from approximately 20% at 2.05 K to 19% at 1.8k. The product of these two factors provides an increase in wall plug power of 20% between 2.05 K and 1.8 K [10]. For the program the temperature effect on the Carnot work was calculated as the ratio of the temperatures. For the Carnot efficiency a linear equation was calculated based on the values at 2.05 K and 1.8 K.

Figure 4 shows the cost and efficiency estimates used for the cryogenic plant as a function of "2 K" power. The steps at 5 kW and 3.8 kW for the 2 K and 1.8 K systems were based on the practical aspect of building and shipping the components [5]. The primary issue is shipping of an assembled cold box by truck. Above these power break points the plant must be split into two sections. While one might consider using plants of different power ratings in order to reduce the cost, such plants might be less than ideal when considering standby (half power) operations, spare parts, engineering design costs, and overall maintenance costs. Based on this the model simply divides the plant into two equal sized plants. The efficiency steps up to match that of the smaller plant.

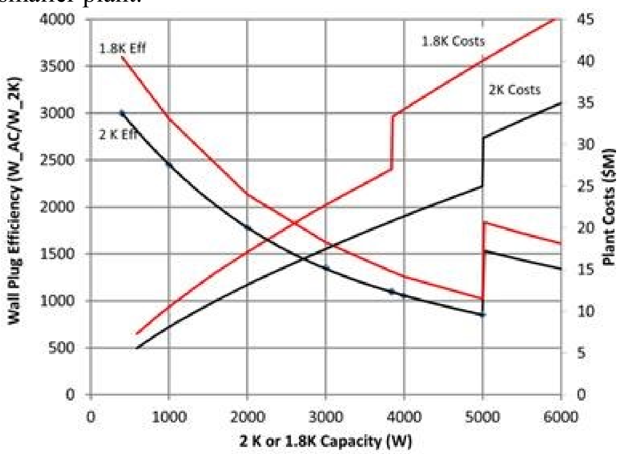


Figure 4: The wall plug efficiency and facility plant procurement costs for a helium refrigerator operated at 2.0 K and 1.8 K respectively.

## *User Interface and Controls*

In addition to the values entered into the input parameters, baseline cost controls, cryogenic heat loads, etc., there are four buttons on the lower right hand corner of the user screen that allow one to write the data from a particular simulation into a tab delimited text file; pause the program; write the input parameter set to a file; and load a set of previously saved input parameters from a file. The pause button is of particular use in that there are portions of the code that overwrite the input parameters array, which (depending on the timing) can make it difficult to change said inputs. It is also useful to click pause, change parameters, display the data graphs then click resume to see the changes to the output parameters. The different screens are accessed by clicking on the tabs at located near the top of the screen. Selecting the ERL button, which is located in the SRF Parameters In cluster, will cause a cluster of ERL parameters to become visible.

# RESULTS

There are three sub-programs that process the data similarly. The first two use frequency scaling of cavity parameters such as shunt impedance, provide cost at a given operating gradient, accelerator energy and beam current as a function of frequency. The third was designed to look at either existing or proposed cryomodule designs including specific cavity shape parameters.

## *Cost as a Function of Frequency*

One approach to the analysis of cost as a function of frequency is to maintain a constant active length of the linac. Figure 5 shows such an analysis where a 2 GeV linac was modeled with 21 cryomodules and a linac total active length of 118 m. In this model, as is often done when performing this type of optimization, cavities are not causal as it relies on a fractional number of cavities per cryomodule. Alternately one could consider using an integer number of cavities per cryomodule, which would limit the model to approximately 10 points for the same parameter sweep.

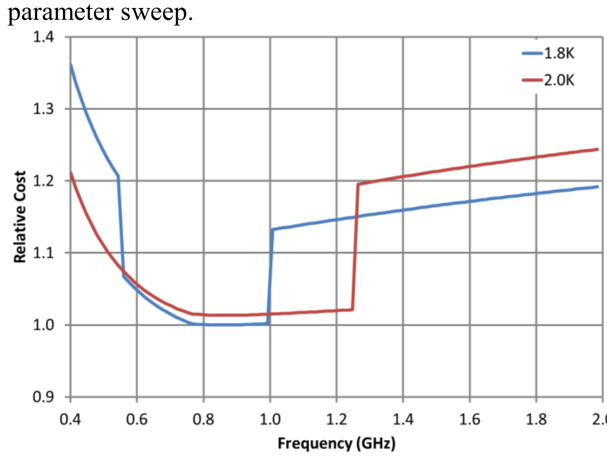


Figure 5: Relative cost of a 118 m active length, 21 cryomodule, 2 GeV linac plus 10 years of electrical power as a function of frequency and temperature.

Alternately, one can use practical cryomodules. For the results shown in Figure 6, the cryomodules were limited to 8 m of active length, resulting in 10 m to 12 m cryomodule lengths. The number of cells per cavity was varied from 4 cells at 500 MHz up to 11 cells above 1800 MHz resulting in cavities that are less than 1.2 m active length for any given cavity. This results in

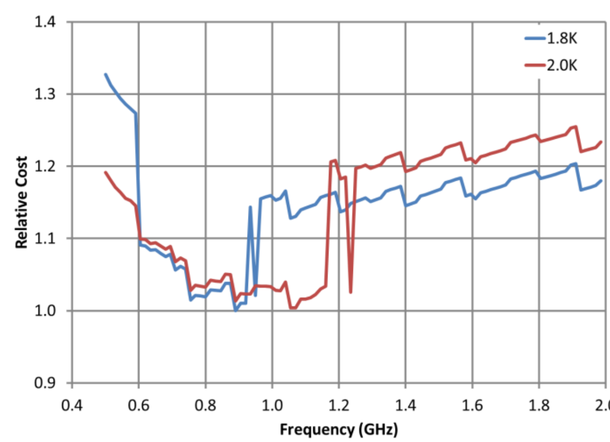


Figure 6: Relative cost of a 2 GeV linac plus 10 years of electrical power as a function of frequency and temperature for 10 – 12 m cryomodules each with a maximum of 6 m of active length and an integer number of cavities.




ISBN 978-3-95450-143-4

quantized steps in the relative costs plots. In these results, the steps are changes in the number of cryomodules. Also as one changes the frequency for a given cryomodule configuration the gradient must be reduced slightly (up to 10%) so as to provide the target machine energy. At lower frequencies the model for $Q_0$ currently employed does not have gradient dependence and thus there is a downward slope in the overall costs (lower cryogenic needs at lower gradients). At higher frequencies the $Q_0$ slope more than makes up for the reduction in gradient and the $Q_0$ losses increase as a function of frequency.

### *Cost as a Function of Gradient*

For this model the program was set up with fixed cryomodule and cavity parameters and by sweeping the gradient, one is able to better understand the cost drivers and implications. In actuality the program is sweeping through the number of cryomodules and calculating the average gradient such that the desired energy is achieved.

Note that if the machine is run off-crest, for a given number of cryomodules the gradient will have to be increased by a factor of $1/\cos(\psi_B)$ in order to provide the design beam energy gain. Figure 7 shows the relative cost of the C100 cryomodule design which was used in the 12 GeV upgrade [11]. The C100 cryomodule contains 8 cavities, each with seven cells operated at 1497 MHz, where each of the cavities has a normalized shunt impedance of 1288 Ω/m and a geometry factor of 280 Ω. This was compared to a cryomodule that could be built out of 6 cavities, of 5 cells each operated at 748.5 MHz. For this model the cavities had a normalized shunt impedance of 644 Ω/m and a geometry factor of 280 Ω.

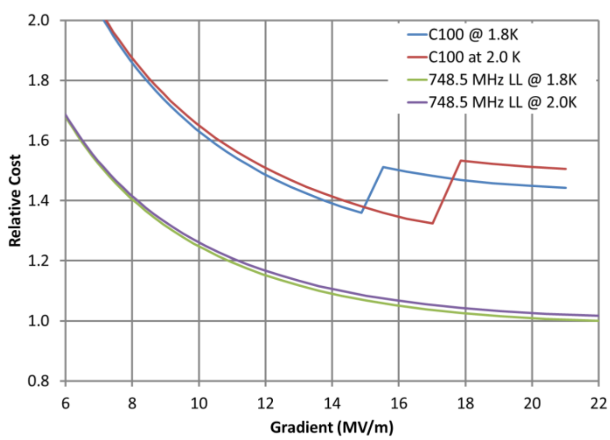


Figure 7: Relative cost of a 2 GeV linac plus 10 years of electrical power as a function of gradient and temperature.

Figure 8 shows the relative cost breakdown for the same C100 cryomodule configuration. One can see that the cost driver at the lower gradients is the cryomodule and accelerator civil construction costs. At higher gradients there is a step increase in cryogenic costs as the system exceeds a 5 kW or 3.8 kW cryogenic plant rating for 2.0 K and 1.8 K operating points respectively. After that point the cost of the cryogenic facility and the 10 year electrical power costs become a significant fraction of the cost.

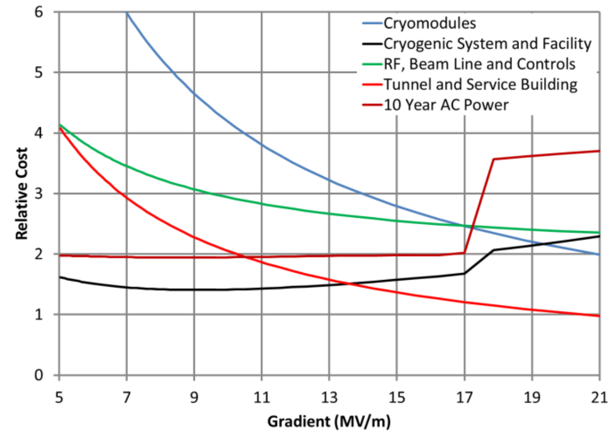


Figure 8: Relative cost breakdown for the components used in determining the cost for the C100 cryomodule based linac operated at 2.0 K.

## MODEL DEFICIENCIES AND FUTURE IMPROVEMENTS

The model used for the results in this paper has a number of issues which still need to be addressed. Also since the current model uses a fixed number for the cryomodule unit cost, it is important to note that cryomodules with different numbers of cavities, couplers, cryogenic distribution systems, and cavity types have different costs. In addition to issues like coupler selection, the program does not take into account the material costs increases that occur when building cryomodules at lower frequencies. This can easily be addressed by using the sweep gradient version of the software and adjusting the cryomodule costs when selecting each of the different types or entering your own variant of a cryomodule.

The $Q_0$ data used for the analysis was taken from vertical tests. Thus there is no accounting for degradations and additional RF losses due to phenomena such as imperfect magnetic shielding, fundamental power coupler losses, and long term degradation due to new field emitters all of which occur when the cavities are installed and operated in a cryomodule. The model does not include high field Q-slope or any distribution function for field emission losses. While the data for the CEBAF C100 production run of 80 cavities, installed in 10 cryomodules, was compared to the model. Further analysis of state of art production data as well as data from past production runs and data from operational machines should allow us to further refine the $Q_0$ models used. Reviewing actual costs for specific systems, hardware and constructions, as well as those included in proposals for new machines should provide us with results that are more in line with reality. In addition to addressing these issues we would like to also include more accurate distributions of gradients into the model which will affect the cryogenic losses.

## CONCLUSIONS

These tools allow one to better understand the tradeoffs relating to the top level design parameters of an SRF linac. They allow one to make adjustments to the baseline costs, cavity parameters, machine packing factors, etc. on the fly and to get a quick feedback as to the impact. The cost estimates for the individual items within the program will need completed on a machine by machine, and location by location basis. Since this describes initial applications of a new program, any use of the results of the simulation in its current state should be done with care. For example, simple things such as inclusion of field emission onset, or Q-slope changes at lower frequencies, can dramatically change the optimum operations frequency, as both would tend to degrade high field operations. Inclusion of high field Q-slope will lead to increases in costs at the higher field levels and may lead to lower optimized field. Additionally, although the baseline cost information is felt to be reasonable, different locations will have different construction and electric power costs. Although we have made good progress in developing the tools for understanding machine cost tradeoffs more work is necessary in order to understand all of the impacts of the different parameters.

## ACKNOWLEDGMENT

The author would like to acknowledge and thank Dana Arenius, Gigi Ciovati, Rao Ganni, and Bob Rimmer, from Jefferson Lab as well as Frank Marhauser from Muons, Inc. for support and discussions related to this topic. Additionally, to thank Gigi Ciovanti for his help in developing the section of the code that calculates $Q_0$ as a function of gradient, cavity parameters and temperature.

## REFERENCES

[1] McIntosh, P., Accelerator Science and Technology Centre, Daresbury, UK, personal communication, May 2009.

[2] ICFA Beam Dynamics Newsletter #60, pp.

[3] Powers, T., "RF Controls Experience with the JLAB IR Upgrade FEL," 2009 ERL Workshop, Ithaca, NY, June, 2009.

[4] Ciovati, G., et. al., "Residual Resistance Data from Cavity Production Projects at Jefferson Lab," IEEE Transactions on Applied Superconductivity, Vol 21, No. 3, June 2011.

[5] Powers, T., "Practical Aspects of SRF Cavity Testing and Operations," Tutorial, SRF Workshop, Chicago, IL, July 2011.

[6] Arenius, D., Thomas Jefferson National Accelerator Facility, Newport News, VA, personal communications, Feb. 2013.

[7] Ganni, R., et. al., "Cryogenic Systems Improvements," Presented at The Thomas Jefferson National Accelerator Science and Technology Review, May, 2008.

[8] V. Ganni, et. al,, "Helium Refrigeration Considerations for Cryo-module design," Proceedings of the 2013 Cryogenic Engineering Conference, Anchorage, AK, June 2013.

[9] Knudsen, et. al., "Process Options for Nominal 2-K Helium Refrigeration System Designs, Advances in Cryogenic Engineering, AIP Conference Proceedings 1434, Spokane, WA, June 2011.

[10] Ganni, R., Thomas Jefferson National Acceleraotr Facility, Newport News VA, personal communications, Sept. 2013.

[11] Pilat, F., "JLAB Upgrade," Presented at Linac 12, Tel Aviv, Israel, Sept. 2012



ISBN 978-3-95450-143-4